Controlling the Critical Behavior of Paranematic to Nematic Transition in Main-Chain Liquid Single-Crystal Elastomers

George Cordoyiannis, Andrija Lebar, Brigita Rožič, Boštjan Zalar, and Zdravko Kutnjak*

Jožef Stefan Institute, P.O. Box 3000, 1001 Ljubljana, Slovenia

Slobodan Žumer

Department of Physics, Faculty of Mathematics and Physics, University of Ljubljana, Jadranska 19, 1000 Ljubljana, Slovenia and Jožef Stefan Institute, P.O. Box 3000, 1001 Ljubljana, Slovenia

Felicitas Brömmel, Simon Krause, and Heino Finkelmann

Institut für Makromolekulare Chemie, Albert-Ludwigs-Universität Freiburg, Freiburg D-79104, Germany

Received September 8, 2008; Revised Manuscript Received January 20, 2009

ABSTRACT: We investigated the paranematic-to-nematic phase transition of nematic main-chain liquid single-crystal elastomers by means of high-resolution ac calorimetry and deuteron quadrupole-perturbed nuclear magnetic resonance. We determined that the cross-linking density strongly affects the thermodynamic response of the system, driving the transition from first order to supercritical via critical point of liquid−vapor type. This result together with recent findings in side-chain liquid crystal elastomers support the universality of such thermodynamic behavior in liquid crystal elastomers. Furthermore, the impact of frozen-in mechanical field during the preparation of samples has been systematically explored in this work. It is shown that the critical behavior can be controlled by both cross-linkers-induced internal random mechanical fields and frozen-in uniform mechanical field applied externally.

I. Introduction

Liquid single crystal elastomers (LSCEs) are materials in which the orientational order of conventional liquid crystals is combined with the elasticity of polymer networks.[1,2] Many interesting properties were expected to emanate from the coupling between nematic liquid crystalline order and elastic deformations[3] including the giant thermomechanical response. This property, explored in various theoretical works,[4−6] makes these materials interesting candidates for various applications, such as sensors, actuators, or artificial muscles.[7,8] To optimize the performance of elastomers in applications it is necessary to accurately determine how smoothly or abruptly they contract or expand as a function of temperature, which is reflected to their phase transition behavior.

The isotropic-to-nematic (I−N) transition of conventional nematic liquid crystals is very well characterized as a weakly first order one since many years ago.[9] On the contrary, in the case of nematic liquid crystalline elastomers the situation was unclear until very recently. In terms of few experimental and several theoretical works a supercritical evolution of the physical properties from paranematic to nematic phase (PN−N) was considered, and it was attributed to either an internal mechanical field conjugate to the order parameter or quenched random disorder effects.[10−22] A possibility to have a discontinuous phase transition behavior in LSCEs was indicated[4,16] but not experimentally explored in a systematic way.

Recently, it was shown that discontinuous or subcritical behavior can be realized, when swelling a supercritical side-chain LSCE (SC-LSCEs) with a significant amount of conventional nematic liquid crystal.[23] Afterward, there was the first direct observation of intrinsic subcritical behavior in SC-LSCEs by means of calorimetry and nuclear magnetic resonance.[24] In the latter it was clearly demonstrated that the thermodynamic response of SC-LSCEs can be controlled by changing a single chemical parameter, namely the cross-linker concentration. By varying the cross-linker concentration the thermodynamic behavior of the system in the vicinity of the PN−N critical point can be tuned from first order to critical and even to supercritical, which is reflected in different temperature profiles of the thermomechanical response.

In the recent years, nematic main-chain LSCEs (MC-LSCEs)[25] have attracted considerable attention due to even stronger thermomechanical response. Few investigations have been already performed on these systems mostly related to the studies of the thermomechanical, stress−strain, and shear response.[26−29] However, systematic studies of the nature of the paranematic to nematic phase transition and the impact of the internal and external mechanical fields on thermodynamical response were not yet carried out. In order to explore this issue in main-chain LSCEs, we performed high-resolution calorimetric and deuterium nuclear magnetic resonance measurements on samples of various concentrations of cross-linkers and samples oriented during the preparation process by different external uniform mechanical stresses. It is shown that both internal and external mechanical fields can significantly influence the nature of the PN−N transition.

II. Materials and Methods

The investigated MC-LSCEs consist of a backbone with siloxane-based chain extenders, rod-like mesogenic molecules and isotropic cross-linkers with five cross-linking points (HD5). A rough two-dimensional schematic representation of such a MC-LSCE network is shown in Figure 1. All samples were prepared using the well established two-step Finkelmann procedure,[30] according to which the second cross-linking step was carried out in nematic phase (at about 330 K) under mechanical load. Various concentrations of cross-linkers were supplied, namely $x = 0.025$, 0.04, 0.06, 0.08,

* Corresponding author.

10.1021/ma802049r CCC: $40.75
Published on Web 02/18/2009

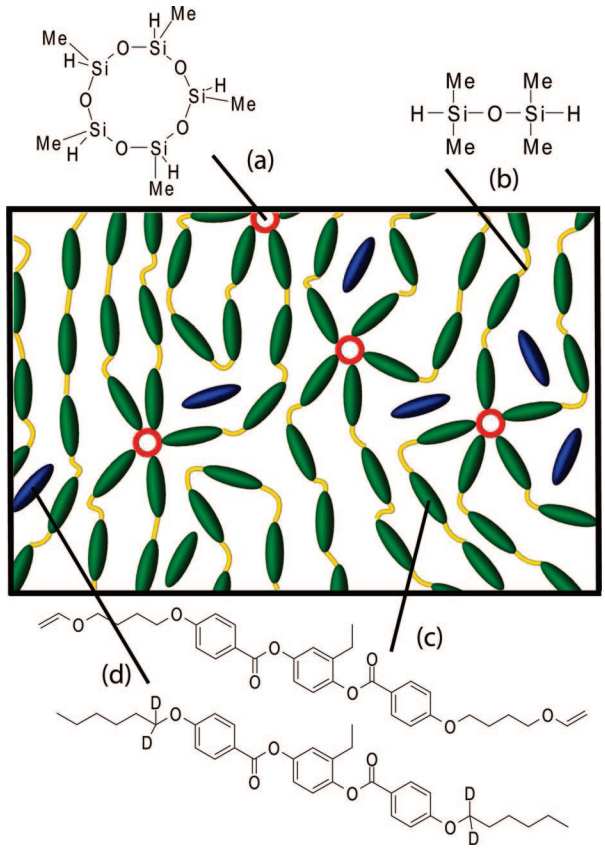

Figure 1. Two-dimensional schematic representation of a nematic main-chain LSCE, consisting of an isotropic cross-linker (a), siloxane-based chain extenders (b), and mesogenic molecules (c). Deuterium labeled probe-mesogens (d) were used only in NMR experiments.

0.12, where x stands for the ratio of the number of cross-linker and mesogen molecules. Additionally, in order to explore the role of sample preparation conditions on the phase transition behavior, samples of same cross-linker concentration ($x = 0.04$) were oriented during the preparation by applying different external mechanical loads of 91 and 24 kPa. Both mechanical loads were above the critical stress threshold required to align the sample. For $x = 0.04$ cross-link density, this critical stress threshold was always less than 10 kPa, as determined in a standard way by comparing measurements of birefringence and NMR spectra of differently stressed LCE samples. So our study was performed exclusively on monodomain samples.

The technique employed for the heat capacity (C_p) measurements is high-resolution ac calorimetry. The temperature dependence of the heat capacity is measured precisely using slow scanning rates, upon heating or cooling. In the principal mode of operation, namely the ac mode, an ac input power is used, causing small oscillations (in the range of mK) of the sample temperature around its mean value. The heat capacity is derived as a function of the amplitude and the frequency of the applied power, as well as the amplitude of the resulting temperature oscillations. In the conventional ac calorimeters, operated only in the ac mode, one can qualitatively distinguish between first (discontinuous) and second order (continuous) phase transitions from the phase of the signal. Nevertheless, since the directly measured quantity is the heat capacity, and not the enthalpy (H), no quantitative values of the latent heat (L) can be provided in case of a first order transition. Our apparatus is a computer-controlled ac calorimeter specially modified to operate in two different modes: the (conventional) ac and the relaxation mode, in order to allow the quantitative determination of latent heat. The ac mode is sensitive only for the continuous changes of the enthalpy $\delta H = \int C_p \, dT$. The relaxation mode is preformed using a linearly ramped power and it yields the effective heat capacity ($C_{p_{eff}}$). As a consequence, it probes both the continuous and discontinuous changes of the enthalpy $\delta H + L = \int C_{p_{eff}} dT$ involved in a phase transition. By performing runs with the two modes and comparing the integrals of the resultant C_p anomalies, one can determine the latent heat of a first order transition. In a case of a continuous or supercritical transition the C_p anomalies obtained from the two modes are identical. The ac calorimetry apparatus as well as the two modes of operation, accompanied by adequate mathematical formulation, have been thoroughly described elsewhere.[31,32]

The samples under investigation were placed in silver cells, taking extra care to leave sufficient free space for their expansion. A very thin layer of Teflon was placed on both top and bottom of the samples, in order to eliminate the possibility of introducing an additional stress via samples sticking to the internal walls of cell. Due to fact that the effective Young modulus of thin Teflon film is at least 1 order of magnitude smaller than that of elastomer the elastomer is almost without resistance stretching the Teflon, which in turn is slipping freely in the cell. After each measurement, the C_p of Teflon and of empty cell were subtracted in order to derive the net C_p of the elastomer. For ac runs the heat capacity data were collected upon cooling, with scanning rates of 0.8 K/h. The typical magnitude of the linear variation of the temperature in relaxation runs was ≈ 0.7 K.

The deuteron NMR spectra were taken at the deuteron Larmor frequency 76.7 MHz using the $(\pi/2)_x-\tau-(\pi/2)_y$—"solid echo" pulse sequence on cooling the samples down from 370 K at cooling rate of 0.1 K/min. We carefully checked that at this cooling rate conditions for equilibrium were met. In addition the temperature was stabilized for 30min before each NMR data taking. These measurements were carried out on a distinct batch of samples with $x = 0.04$, 0.08, and 0.12. Each sample was arranged into a double-layered sandwich with dimensions 25 mm × 8 mm × 0.6 mm. In our geometry the samples's long edge, the nematic director, and spectrometer field were all pointing vertical. The sample was clamped at both ends and hung inside a detection coil. The top clamp was fixed inside the probehead, whereas the lower clamp with its small weight (3 g) assured proper straightening of the sample; i.e., no impact of the macroscopic sample curvature on the resulting NMR spectra was detected. We used "soft" clamps, which allowed the sample to shrink and expand in the direction perpendicular to the nematic director in an unhindered fashion. The sample thus maintained a perfect rectangular shape and uniform director orientation at arbitrary deformations induced by a temperature change.

The deuterium NMR sensitivity was achieved by doping the LSCE samples with a small amount (ranging between 8 and 11 mass percent) of selectively deuterium labeled probe-mesogens. The impact of concentration of NMR probe mesogens was checked independently by varying their concentration. In the used range of probe mesogen concentration between 8 to 11 mass percent the phase transition behavior was practically identical to that of main-chain LSCEs samples doped with much smaller amount of probe mesogens, thus excluding the impact of NMR probe mesogens on the nature of the paranematic to nematic phase transition. This is not surprising because the probe mesogens used in our NMR experiments are very similar to mesogens originally found in already investigated main-chain LSCEs (see Figure 1). Still, the doping resulted in a shift of the phase transition temperature of main-chain LSCEs by about 10−15 K toward higher temperatures, which is due to the higher transition temperature (418 K) of bulk probe mesogens.

III. Experimental Results and Discussion

The temperature profiles of ΔC_p for all five concentrations are given in Figure 2. The solid and open symbols represent the data obtained with the ac and relaxation mode, respectively. In all cases the ΔC_p temperature profile is derived after subtracting a background. The data of different runs have been shifted along the ΔC_p axis for clarity. In low concentrations the C_p anomalies obtained in ac and relaxation runs differ

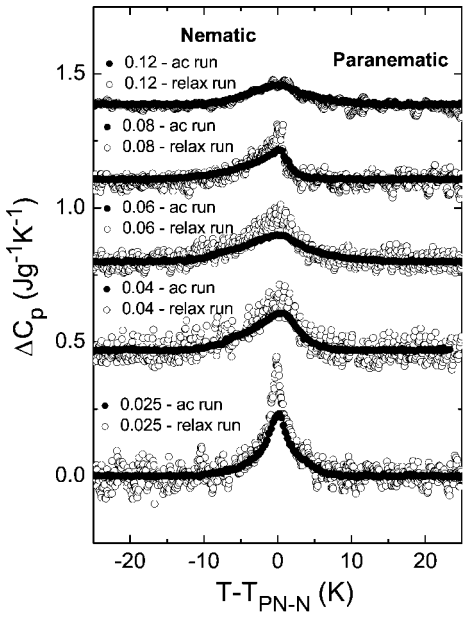

Figure 2. ΔC_p data obtained in the relaxation and ac runs as functions of temperature for five different concentrations of MC-LSCEs: x = 0.025, 0.04, 0.06, 0.08, and 0.12.

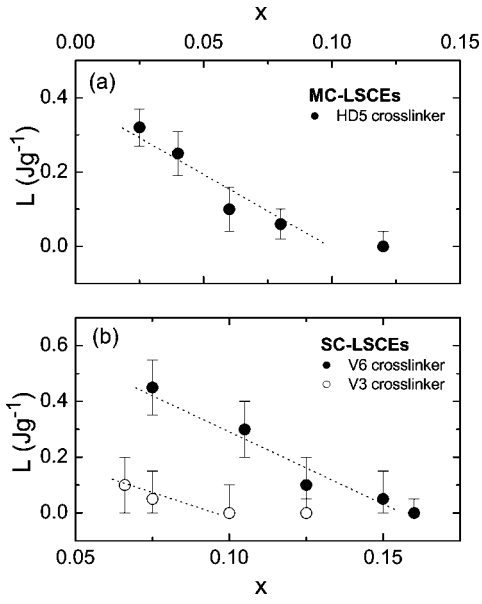

Figure 3. The latent-heat dependence on cross-linker concentration for (a) MC-LSCEs and for (b) SC-LSCEs (data taken from ref 24). Dotted lines are simple guides to the eye.

significantly. This clearly demonstrates the presence of nonzero latent heat and implies a first order transition. It is noteworthy that the latent heat is released in a wide temperature range of several degrees where PN and N phases coexist, contrary to conventional nematic liquid crystals where the phase coexistence range is few tens of mK. With increasing cross-linker concentration the difference between the ac and relaxation modes becomes smaller and the latent heat gradually decreases. Finally, it vanishes for high concentrations (e.g., x = 0.12), where a smooth supercritical-like PN−N evolution is realized.

In parts a and b of Figure 3, the latent heat versus x is compared for MC-LSCEs with isotropic cross-linkers (this work) and SC-LSCEs with a rod-like (V6) and a point-like (V3) cross-linker, taken from ref 24. Note that due to the different cross-linking topology in case of MC-LSCEs and SC-LSCEs the x stands only for an analogous but not for the same quantity (see[24] for definition of x in case of SC-LSCEs). Nevertheless, the thermodynamic behavior of MC-LSCEs is analogous to the one observed in SC-LSCEs. Here, with increasing concentration of cross-linkers the latent heat gradually disappears indicating the conversion of the first order transition (at lower x values) to a supercritical one (at higher x values) via an isolated liquid−vapor type critical point.

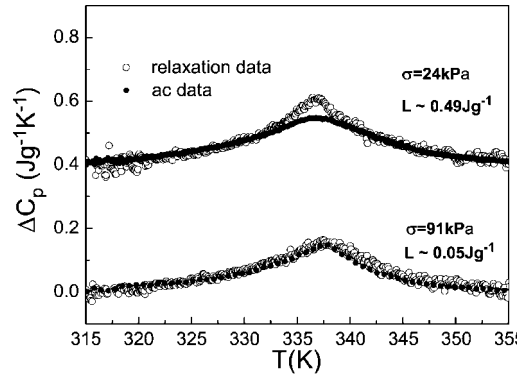

Figure 4. ΔC_p data determined in the relaxation and ac runs as functions of temperature for samples of cross-linker concentration x = 0.04, prepared under two different external mechanical loads.

In Figure 4 the excess C_p temperature profiles obtained in ac and relaxation runs are plotted for two samples of the same cross-linker concentration, that were stretched during the second cross-linking step with two different external mechanical loads, 24 and 91 kPa respectively. The sample prepared using smaller value of the external mechanical field exhibits slightly sharper PN−N heat capacity anomaly involving latent heat of 0.49 ± 0.07 J/g. In contrast, the sample prepared under stronger external mechanical field exhibits more suppressed supercritical like PN−N C_p anomaly, with nearly zero latent heat within the experimental error of ± 0.07 J/g. Therefore, the external mechanical stresses used during the preparation of the sample seems to play an analogous role in changing the nature of the PN−N transition in main-chain LSCEs as internal stresses related to different cross-link density.

We show a selection of our NMR results in Figure 5. A typical recorded NMR spectrum is a doublet with its splitting proportional to the local order parameter. In most of our spectra we observe a well separated doublet. We note, however, that the typical doublet lines are much broader than the ones obtained in spectra of side-chain LSCEs in our previous studies.[23,24] This could be so for several reasons, such as, larger network heterogeneity or lower degree of nematic domain alignment in main-chain LSCEs, but most probably, broader lines are a consequence of slow dynamics encountered in main-chain LSCEs. A mesogen in a main-chain LSCE is attached at its both ends to the rest of the polymer backbone, so its dynamics is expected to be considerably slower when compared to a mesogen in a side-chain LSCE that is only attached at one end. The fact that network mesogens and probe-mesogens in a main chain LSCE are considerably larger than the ones in side-chain LSCEs adds to this effect.

The result of a slower mesogen dynamics and therefore less averaging of the spectral lines in main-chain LSCEs are broader spectral features and worse spectral resolution when compared to side-chain LSCEs. This is particularly noticeable in high temperature spectra where typical order parameter values may be less than 0.01. In NMR spectra of side-chain LSCEs one could mostly resolve a doublet even at these low values of S. On the contrary, in the present study on main-chain LSCEs in most cases the doublet can not be resolved in high-temperature NMR spectra; it is only resolved in the spectra of the sample with highest cross-linker concentration.

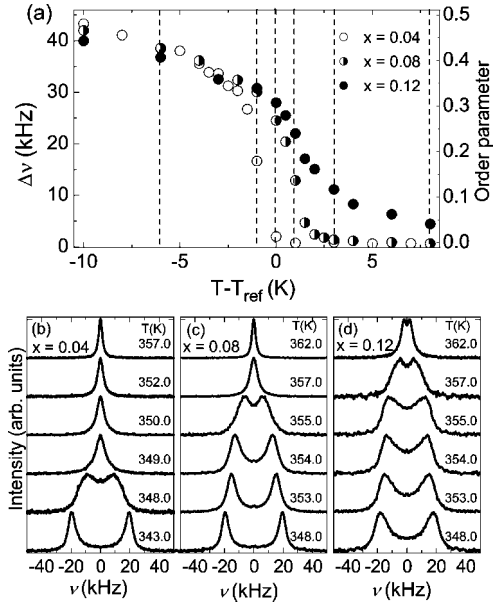

Figure 5. (a) Temperature dependencies of deuterium NMR spectrum doublet splitting for three LSCE samples with different cross-linker concentration x. The average local order parameter corresponding to the doublet frequency splitting is assigned to the right axis. The reference temperature is $T_{ref} = 349$ K for $x = 0.04$ and $T_{ref} = 354$ K for both $x = 0.08$ and $x = 0.12$. These values were chosen so that T_{ref} matches T_{PN-N} of the $x = 0.04$ sample and the $S(T)$-dependencies of all samples overlap at low temperatures. Selected NMR spectra for $x = 0.04$ (b), $x = 0.08$ (c), and $x = 0.12$ (d) at temperatures denoted with dashed lines in part a are displayed with the actually measured temperature values.

Despite the overlapping of doublet lines in high-temperature spectra, resulting in a merging of the doublet into a single detectable spectral line, we could fit all the high-temperature spectra with a doublet of Lorentzians and extract the average value of the local order parameter. At lower temperatures the spectral lines acquire peculiar shapes that reflect a distribution of local order parameter in the vicinity of the phase transition temperature. At even lower temperatures a distribution of the domain alignment directions is reflected in the typical asymmetric inward broadening of doublet lines. Thus we extracted the average value of the order parameter at lower temperatures by fitting only the outer parts of the spectral lines by Lorentzians. The obtained $S(T)$ dependencies for the three samples are shown in Figure 5a. We note that we shifted the temperature scale of the $x = 0.04$ sample by $+5$ K, so that all $S(T)$ dependencies overlap at low temperatures and a better comparison is possible. We are allowed to do so, since the shift of the phase transition temperature is among other factors strongly influenced by the amount of probe-mesogens in LSCE, extracted sol content, and other parameters subject to variation during the sample preparation.

The diagram in Figure 5a offers us a qualitative confirmation of what the calorimetric measurements demonstrate. One can clearly observe how increasing the cross-linker concentration in main-chain LSCEs results in a more continuous (i.e., supercritical) evolution of the phase transition. The $S(T)$ dependence of the $x = 0.04$ sample is steep and discontinuous-like, the $S(T)$ dependence for the $x = 0.12$ is relatively flat, and the results for the $x = 0.08$ sample fill well the gap between the two extreme cross-linker concentrations. For a more direct comparison, in parts b−d of Figure 5 we show a selection of NMR spectra at several different temperatures in the vicinity of phase transition for $x = 0.04$, $x = 0.08$, and $x = 0.12$, respectively. One can clearly observe that the temperature interval, in which the spectrum transforms from a narrow paranematic into a broad nematic doublet, increases with the increasing concentration of the cross-linkers. Particularly noticeable is the well-separated doublet of the $x = 0.12$ sample at high temperatures, indicating a relatively high paranematic order, which is a feature of a strongly supercritical transition.

We note, that unlike in our previous studies, here we can not calculate moments of individual NMR spectral lines, which would make it possible to quantitatively determine the degree of below- or supercriticality of the phase transition in main-chain LSCEs.[23,24] The reason is that the calculated moments are subject to large errors, since the doublet spectral lines heavily overlap, particularly in the paranematic phase. Therefore, the confirmation of results of calorimetric measurements by the deuterium NMR spectroscopy in this study should be regarded as qualitative.

IV. Conclusions

We performed a systematic study of the PN−N phase transition of main-chain LSCEs by means of ac calorimetry and deuteron quadrupole-perturbed nuclear magnetic resonance. Our experiments clearly show the existence of a liquid−vapor type critical point in the temperature-cross-link density phase diagram of main-chain LSCEs. Specifically, on increasing the cross-links concentration the nature of the phase transition changes from the first order type (subcritical) to continuous (at the critical point) and then to supercritical. According to the theory of critical phenomena, such a sequence is anticipated whenever a field conjugated to the order parameter exits and its strength is gradually increased across its respective critical value. The existence of the "critical point" implies that the low temperature nematic phase possesses the same symmetry as the high temperature phase. In LSCEs it is the local mechanical field which assumes the role of the conjugate field. Therefore it is straightforward to conclude that an increase in the cross-link density results in an increase of the strength of the local mechanical field. Such a behavior has been demonstrated previously for side-chain systems[23] and in this paper for main-chain systems, implying its universality for LSCEs in general.

High-resolution calorimetric measurements on samples oriented during the preparation process by different external uniform mechanical fields show that, in addition to the local mechanical fields, the external mechanical fields can also significantly influence the nature of the PN−N transition in main-chain LSCEs.

Similar to some other systems,[33] the proximity of the critical point allows enhancement of some specific mechanical properties. In particular, by varying the cross-linker concentration or the external uniform mechanical field during the sample preparation process in the vicinity of the PN−N critical point, the temperature profiles of the spontaneous elongation/contraction can be tuned to an on−off, intermediate or continuous type response, which could be tailored depending on application.

Note Added After ASAP Publication. This article was published ASAP on February 18, 2009 with refs 30−33 cited incorrectly in the text. The correct version was published on February 26, 2009.

Acknowledgment. This research was supported by the Slovenian Office of Science Project No. J1-9368 and by EU (HPRN-CT-2002-00169). A.L. gratefully acknowledges the support of an Alexander-von-Humboldt research fellowship.

References and Notes

(1) Warner, M.; Terentjev, E. M. *Liquid Crystal Elastomers*; Oxford University Press: New York, 2007.
(2) Warner, M.; Terentjev, E. M. *Prog. Polym. Sci.* **1996**, *21*, 853.

(3) de Gennes, P. G. C. R. *Acad. Sci. (Paris)* **1975**, *281*, 101.
(4) Verwey, G. C.; Warner, M. *Macromolecules* **1997**, *30*, 4196.
(5) Terentjev, E. M. *J. Phys: Condens. Matter* **1999**, *11*, R239.
(6) Xing, X.; Radzihovsky, L. *Phys. Rev. Lett.* **2003**, *90*, 168301.
(7) Lehmann, W.; Skupin, H.; Tolksdorf, C.; Gebhard, E.; Zentel, R.; Kruger, P.; Losche, M.; Kremer, E. *Nature* **2001**, *410*, 447.
(8) Shenoy, D. K.; Thomsen, D. L.; Srinivasan, A.; Keller, P.; Ratna, B. *Sensor Actuators A* **2002**, *96*, 184.
(9) Marynissen, H.; Thoen, J.; Van Dael, W. *Mol. Cryst. Liq. Cryst.* **1983**, *97*, 149.
(10) Kaufhold, W.; Finkelmann, H.; Brand, H. R. *Makromol. Chem.* **1991**, *192*, 2555.
(11) Disch, S.; Schmidt, C.; Finkelmann, H. *Makromol. Rapid. Commun.* **1994**, *15*, 303.
(12) Brand, H. R.; Kawasaki, K. *Macromol. Rapid Commun.* **1994**, *15*, 251.
(13) Pereira, G. G.; Warner, M. *Eur. Phys. J. E* **2001**, *5*, 295.
(14) Greve, A.; Finkelmann, H. *Macromol. Chem. Phys.* **2001**, *202*, 2926.
(15) Clarke, S. M.; Hotta, A.; Tajbakhsh, A. R.; Terentjev, E. M. *Phys. Rev. E* **2001**, *64*, 061702.
(16) Selinger, J. V.; Jeon, H. G.; Ratna, B. R. *Phys. Rev. Lett.* **2002**, *89*, 225701.
(17) de Gennes, P. G.; Okumura, K. *Europhys. Lett.* **2003**, *63*, 76.
(18) Selinger, J. V.; Ratna, B. R. *Phys. Rev. E* **2004**, *70*, 041707.
(19) Petridis, L.; Terentjev, E. M. *Phys. Rev. E* **2006**, *74*, 051707.
(20) Petridis, L.; Terentjev, E. M. *J. Phys. A: Math. Gen.* **2006**, *39*, 9693.
(21) Levstik, A.; Filipic, C.; Kutnjak, Z.; Careri, G.; Consolini, G.; Bruni, F. *Phys. Rev. E* **1999**, *60*, 7604.
(22) Feio, G.; Figueirinhas, J. L.; Tajbakhsh, A. R.; Terentjev, E. M. *Phys. Rev. B* **2008**, *78*, 020201.
(23) Lebar, A.; Kutnjak, Z.; Žumer, S.; Finkelmann, H.; Sanchez-Ferrer, A.; Zalar, B. *Phys. Rev. Lett.* **2005**, *94*, 197801.
(24) Cordoyiannis, G.; Lebar, A.; Zalar, B.; Žumer, S.; Finkelmann, H.; Kutnjak, Z. *Phys. Rev. Lett.* **2007**, *99*, 197801.
(25) Donnio, B.; Wermter, H.; Finkelmann, H. *Macromolecules* **2000**, *33*, 7724.
(26) Wermter, H.; Finkelmann, H. *e-Polym.* **2001**, *13*, 1. http://www.e-polymers.org.
(27) Bispo, M.; Guillon, D.; Donnio, B.; Finkelmann, H. *Macromolecules* **2008**, *41*, 3098.
(28) Rogez, D.; Brandt, H.; Finkelmann, H.; Martinoty, P. *Macromol. Chem. Phys.* **2006**, *207*, 735.
(29) Krause, S.; Zander, F.; Bergmann, G.; Brandt, H.; Wermter, H.; Finkelmann, H. *C. R. Chimie* **2009**, *12*, 85.
(30) Küpfer, J.; Finkelmann, H. *Makromol. Chem. Rapid. Commun.* **1991**, *12*, 717.
(31) Yao, H.; Ema, K.; Garland, C. W. *Rev. Sci. Instrum.* **1998**, *69*, 172.
(32) Kutnjak, Z.; Kralj, S.; Lahajnar, G.; Žumer, S. *Phys. Rev. E* **2003**, *68*, 021705.
(33) Kutnjak, Z.; Petzelt, J.; Blinc, R. *Nature* **2006**, *441*, 956.

MA802049R